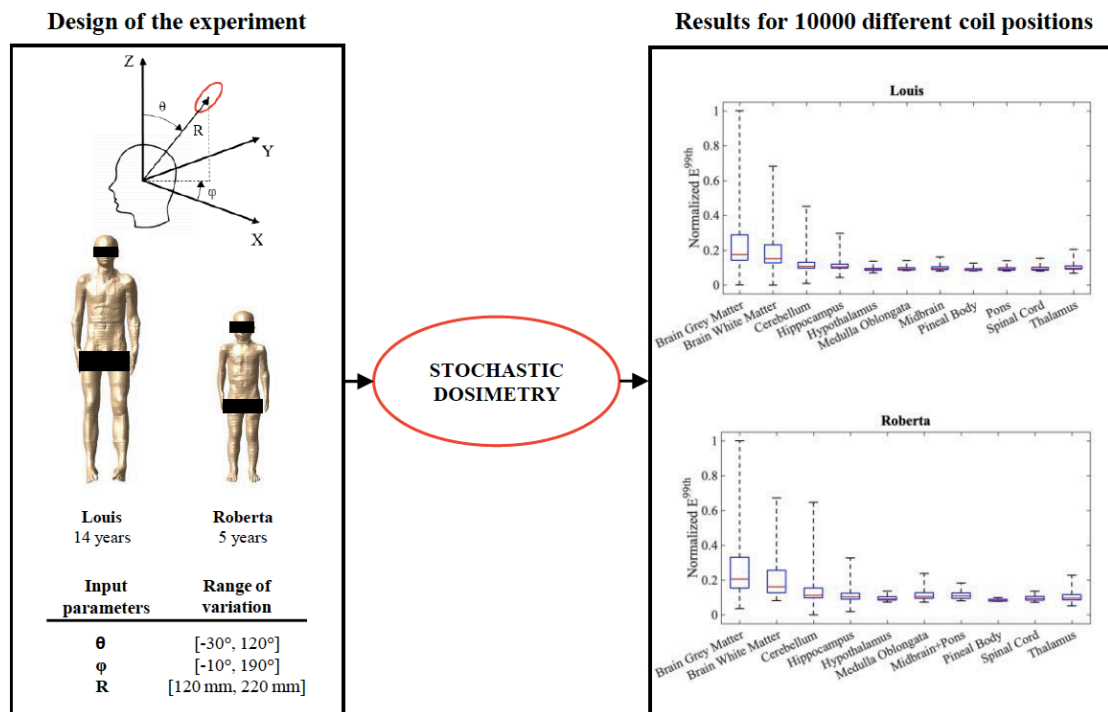


Influence of low frequency Near-Field Sources Position on the Assessment of Children Exposure Variability using Stochastic Dosimetry

Marta Bonato, *Student Member, IEEE*, Emma Chiamello, Serena Focchi, Gabriella Tognola, Paolo Ravazzani, *Member, IEEE* and Marta Parazzini, *Member, IEEE*



Assessment of children exposure variability due to the position of a low frequency near-field source using stochastic dosimetry.

Take-Home Messages

- The stochastic dosimetry approach permitted to evaluate the assessment of children exposure variability due to the position of a low frequency near-field source with low computational efforts
- The method was useful for individuating the source positions area, where the source could cause the highest levels of exposure
- The target biological application is the evaluation of children exposure level due to the common use of domestic appliances, considering the variability of a real exposure scenario
- The work permitted to expand the knowledge about the low frequency near-field sources children exposure, not limiting it only on some worst-case scenario hypothesis

Influence of low frequency Near-Field Sources Position on the Assessment of Children Exposure Variability using Stochastic Dosimetry

Marta Bonato, *Student Member, IEEE*, Emma Chiaramello, Serena Fiocchi, Gabriella Tognola,
Paolo Ravazzani, *Member, IEEE* and Marta Parazzini, *Member, IEEE*

Abstract The objective of the present work was to assess the children exposure variability due to low frequency near-field sources using an approach based on stochastic dosimetry. These scenarios represent a topic of high interest, because it was found that domestic appliances could be relevant for children exposure level. In details, in this paper the exposure of two child models to a hairdryer model was evaluated. Following the ICNIRP guidelines, the electric field amplitudes induced in specific tissues composing the central nervous system and the peripheral nervous system were analyzed. The analysis of the results permitted to highlight a high exposure variability depending on the near-field source position and to individuate the regions where the source could cause the highest levels of exposure, not limiting the analysis only to some worst-case exposure scenarios.

Keywords — Children Exposure, ELF-MF, Near-field source, Stochastic Dosimetry

I. INTRODUCTION¹

SINCE late 1970, the exposure to extremely low frequency magnetic field (ELF-MF, 40-800 Hz) was intensively investigated in environmental epidemiologic studies, as possible health risk factor for childhood leukemia [1]. It was indeed found in several meta-analysis that the risk of childhood leukaemia's onset increased for daily average exposure above 0.4 μT [2-4], although the reason of this correlation is still uncertain [5]. This risk possibility led the International Agency for Research on Cancer (IARC) in 2002 to classify ELF-MF as "possibly carcinogenic to humans" based on "limited evidence of carcinogenicity in humans" and "inadequate evidence of carcinogenicity in experimental animals" [6]. A lot of studies around the world have been therefore conducted to investigate on the level of the magnetic field exposure both in indoor and outdoor situations and to know the possible different factors that influence this exposure [7-10]. The most recent European studies were carried in Italy and in Switzerland by the ARIMMORA project [11-13] and in France by the EXPERS project [14], measuring magnetic field amplitudes through personal dosimeters worn by the children. The measurements signals of these studies

suggested that as well as the traditional power lines (which are typically the first source investigated) also other sources (such as domestic appliances), could be relevant for the children exposure level. This was as well supported by the work of Leitgeb et al. (2008) [15], where it was investigated the magnetic fields emitted by more than 1000 electrical appliances in the 5 Hz to 2 kHz range and it was found that magnetic field levels may be much higher than previously reported. Furthermore, in the work conducted by Schüz [16] in Germany, the data suggested that one-third of total exposure to ELF-MF could be attributed to personal appliance use. For these reasons during the years, the exposure levels caused by different domestic electrical appliances were investigated in other measurements studies, as reported in [17-19]. Furthermore, efforts have been made for describing accurately the magnetic field around the different electrical appliances in order to evaluate possible exposure hazards by numerical approaches [20-24]. Specifically, it was underlined that a full geometry-based numerical modeling of a real magnetic source (e.g., the motor of the electronic appliance) is too complex to permit its application to the intended dosimetry investigation. For this reason, simple numerical source models such as the current loop, coil and a magnetic dipole moment were often used for investigating the inhomogeneous magnetic field dosimetry in the low frequency range. For example, in the work of Nishizawa et al. [22], the accuracy of a simple current loop as equivalent source model was investigated to simulate the magnetic field distribution of a real electronic appliance. In the paper of Cheng et al. [23], the magnetic field of small hand-held appliances was modelled using a magnetic dipole and the induced currents were calculated in a model of the human head. At last, in the paper of Christ et al. [24], the exposure of adults, children and pregnant women due to domestic induction cooktops were evaluated, using as model ten concentric coils. Although efforts have

This research is supported by the French National Research Program for Environmental and Occupational Health of ANSES (2015/1/202): Project ELFSTAT - In depth evaluation of children's exposure to ELF (40 - 800 Hz) magnetic fields and implications for health risk of new technologies, 2015-2019.

M. Bonato, E. Chiaramello, S. Fiocchi, G. Tognola, M. Parazzini and P. Ravazzani are with the Institute of Electronics, Computer and Telecommunication Engineering (IEIIT), CNR, Milano, Italy (e-mail: marta.bonato@ieiit.cnr.it; emma.chiaramello@ieiit.cnr.it; serena.fiocchi@ieiit.cnr.it; gabriella.tognola@ieiit.cnr.it; paolo.ravazzani@ieiit.cnr.it; marta.parazzini@ieiit.cnr.it).

M. Bonato is also with the Department of Electronics, Information and Bioengineering (DEIB), Politecnico di Milano, Italy.

been made, these works still presented some limitations and provided an exposure assessment limited only on some specific cases (typically the worst exposure scenario). Assessing the variability of children exposure to near-field sources in large number of the possible real and highly variable scenarios still represented a challenging task. In fact, an intrinsic variability of the parameters that influence the exposure is present, as the children age, the tissues dielectric parameters and in particular the source position, due to the inhomogeneity of the analyzed magnetic fields.

In some previous studies both at low and high frequency [25-27], for providing a better description of the exposure level, it was used the well know stochastic dosimetry approach based on the Polynomial Chaos theory (PC) [28]. The PC is a technique that combines electromagnetic computational techniques (i.e. deterministic dosimetry) and statistics to build surrogate models for obtaining the distribution of the quantity of interest (the induced electric field amplitude, for instance). The purpose of the following paper is to use the same procedure for evaluating the case of a child exposed to a low frequency near-field source, varying the source position to assess the exposure variability. In this way, it will be possible to evaluate exactly how much the position of the device can affect the exposure level and to identify the source positions with major risk of high exposure levels. In fact, as it is reported in the paper of Cheng et al. [23], in the case of domestic appliances, where the magnetic flux densities rapidly decrease with the distances, the nearest positions of the source to the subject could affect more the exposure level than the farthest positions, which have almost field levels as the ambient field levels. In this work, two different child models were used and a hairdryer was considered as a near-field source, modelled by a simple coil, using the data from the European project ARIMMORA [11]. For each child model, the PC surrogate models calculated the electric field amplitudes induced in specific tissues, following the ICNIRP International Committee of Non-Ionizing Radiation Protection guidelines [29]. At the end, statistical and global analysis were conducted to obtain the variability assessment caused by the near-field source position.

II. METHODS AND PROCEDURES

To assess the exposure variability due to a near-field source, the amplitude of the electric field induced in peripheral nervous system (PNS) and central nervous system (CNS) of two child models was calculated varying the position of the hair dryer respect to the child head using surrogate models based on PC theory.

The schematic view of the exposure scenario and the two high-resolution child models are presented in Fig.1. As it can be seen, the first model was Louis, a 14 years old male boy model, whereas the second one was Roberta, a 5 years old female child model, both the models come from the Virtual Classroom family [30]. For both the cases, the hair dryer was modelled by a coil (shown in red in Fig.1).

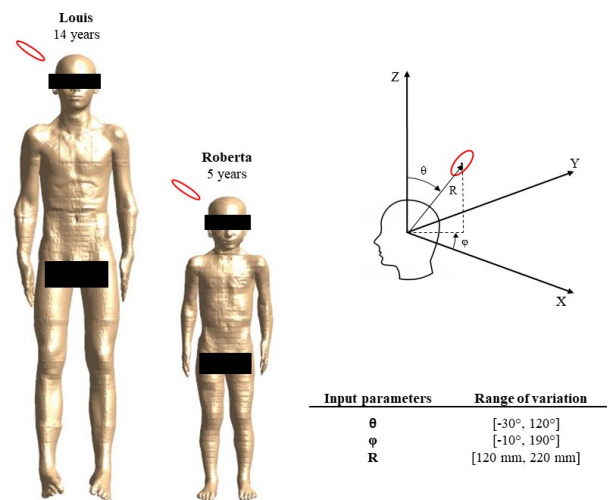


Fig. 1. Schematic view of the exposure scenario: On the left, the two child models utilized from the Virtual Classroom. On the right, the view of the reference axes system and the considered input parameters with the corresponding ranges of variation.

The three input parameters necessary to set the coil position respect to the child head are described in Fig.1. In detail, the two angles φ and θ described the coil rotation around the child head and the parameter R represented the distance between the head and the coil. The variation ranges of the three inputs were: for the angle θ , which is the rotation respect to z axis in the sagittal plane, between -30° and 120° , for the angle φ , which is the rotation in the transversal plane, between -10° and 190° and for the distance R between 12 cm to 22 cm from the head central point.

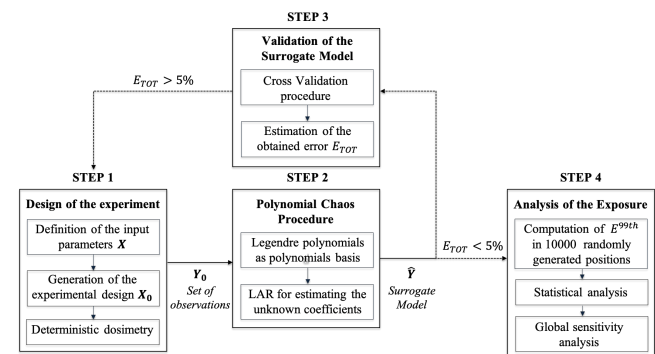


Fig. 2. Flow chart of the experimental procedure.

In Fig.2, it is shown the flow chart utilized for evaluating the child exposure variability due the different hairdryer positions. The same procedure was previously tested and validated in the level exposure assessment for both high and low frequency scenarios [25-27]. The procedure is composed by four step, which will be described in details in the following paragraphs. Briefly, the first step, “Design of the Experiment”, involved the use of the classic deterministic dosimetry for evaluating a minimum set of X_0 experimental observations for calculating the values of the variable of interest Y_0 , needed to build the surrogate model. The second step, “Polynomial Chaos Procedure”, was focused on the development of surrogate models with stochastic dosimetry based on PC theory. The third step,

“Validation of the Surrogate Model”, consisted on the use of a cross validation procedure for validating the obtained models and for defining the minimum number N of simulations necessary to achieve an acceptable error. At the end, in the fourth step, “Analysis of the Exposure”, the surrogate models were used to calculate the 99th percentile value of root mean square induced electric field (indicated from here on as E^{99th}) in the tissues of interest, following the ICNIRP guidelines [29] in order to evaluate the exposure variability assessment to a near-field source.

1. Design of the Experiment

As it can be seen from step 1 of the flow chart in Fig.2, the detection of the input parameters and the definition of their joint probability functions are the first choices necessary for obtaining the experimental design X_0 and thus for applying the PC theory. As told before, the three input parameters ϕ , θ and R were used in the present work to describe the reciprocal position between the child head and the coil. Although it was decided the variation ranges of the three input parameters (as shown in the table of Fig.1), no assumptions were made about the most probable position of the hairdryer in order to avoid losing generality. Thus, uniform distributions were hypothesized for the three input. Successively, a Latin hypercube sampling (LHS) method [31] was applied on the obtained joint probability density function for generating the experimental design X_0 . At this point, the variable of interest Y_0 (i.e. E^{99th}) was evaluated in the simulation platform Sim4Life using deterministic dosimetry; in particular, the magneto quasi-static low frequency solver was used. In details, at low frequency range the magnetic vector potential A is decoupled from the electric field E , because the relevant dimensions of the computational domain are significantly smaller than the free space wavelength, thus A can be calculated using the Biot-Savart's law. Moreover, since in the human body the displacement current is neglected with respect to the conduction current in this exposure condition, E can be calculated from the scalar potential Φ by:

$$-\nabla \cdot \sigma \nabla \Phi = j \omega \nabla \cdot (\sigma A) \quad (1)$$

where σ is the tissue conductivity, ω is the angular frequency and the finite element method is used to solve for Φ . In all the simulations, both the child models were discretized with a grid resolution of 1 mm for having a sufficient discretization of all the tissues examined, following the parameters imposed in the previous work of Chiamarello et al. [26]. The dielectric properties of permittivity and conductivity values were selected according to the data presented in literature [32-34]. The coil dimension was chosen according to data collected in the ARIMMORA project [11], based on real magnetic field measurements emitted by a hairdryer device. For this reason, the diameter of the coil was set at 38.35 mm. The frequency was set to 50 Hz, whereas the coil current was set to an arbitrary current of 1 A. At the end, the computed output variable Y_0 was the previous cited E^{99th} calculated in the tissues of interest, following the metric adopted by the ICNIRP [29]. In specific, the E^{99th} was evaluated for each tissue that composed the central nervous system (CNS) and

for the peripheral nervous system (PNS). In particular, eleven tissues composed the CNS in the Louis model: brain grey matter, brain white matter, cerebellum, hippocampus, hypothalamus, medulla oblongata, midbrain, pons, pineal body, spinal cord and thalamus. For the Roberta model, the CNS tissues were the same, except that midbrain and pons were considered together, as a unique tissue. Optical nerves and spinal nerves composed instead the PNS for both the child models. The set of Y_0 values were successively used to build the surrogate models using the PC theory.

2. Polynomial Chaos Procedure

The problem of surrogate modeling for EMF exposure can be represented as:

$$\hat{Y} = M(X_0) \quad (2)$$

where X_0 denotes the M dimensional input vector from the input parameters that influence the exposure scenario (in this case, the three input parameters in Fig.1) and \hat{Y} represents the quantity of interest (in this case, E^{99th}) obtained with significantly lower computational cost in respect to deterministic dosimetry. Among the different non-intrusive approaches that can be used to build surrogate models, in this work it was chosen the polynomial chaos (PC) theory, which is a spectral method, where the approximation of the output \hat{Y} through its spectral representation has the form:

$$\hat{Y} = M(X_0) = \sum_0^{P-1} \alpha_j \psi_j(X_0) + \varepsilon \quad (3)$$

Where \hat{Y} is the system output, X_0 is the random input vector made of the chosen input parameters X , ψ_j are the multivariate polynomials belonging to $\Psi(X)$, α_j are the unknown coefficients to be estimated, ε is the error due to truncation and P is the size of the polynomial basis $\Psi(X)$. Each multivariate polynomial ψ_j is built as tensor product of univariate polynomials orthogonal with respect to the probability density function of each input parameter. More details about the PCE theory can be found in [25, 31].

As it is shown in step 2 of Fig.2, the first part of the polynomial chaos procedure was the selection of the proper polynomial basis. In this work, the Legendre polynomials were selected respecting the input probability density functions, which were uniformly distributed. The second part of the procedure was focused in calculating the unknown coefficients. In specific, it was used the Least Angle Regression algorithm [35], based on least-square regression on the output observations Y_0 calculated with deterministic dosimetry. For implementing the PC procedure and obtaining the surrogate models of the variables of interest, the software “UQLab: The Framework for Uncertainty Quantification” [36] was here used.

3. Validation of the Surrogate Model

The validation of the obtained surrogate models was performed using a leave-one-out cross-validation technique, based on a previous work of Chiamarello et al. [26]. The method is used to reduce at minimum the size of the experimental design. It consisted in using all the determinist dosimetry simulations except one to build each surrogate

model. The obtained surrogated model was then utilized to predict the output value \hat{Y}_i of the excluded simulation. At last, it was performed the comparison between the result obtained from the surrogate model (\hat{Y}_i) and the result obtained using determinist dosimetry ($Y_{0,i}$). In this way, the error calculated is in the form:

$$E_i = \left(\frac{Y_{0,i} - \hat{Y}_i}{Y_{0,i}} \right)^2 \quad (4)$$

The procedure is repeated recursively for all the simulations and summing all the errors of the leave one out process. The final percentage error is thus obtained in the form:

$$E_{tot} = 100 * \frac{1}{N} \sum_{i=1}^N E_i \quad (5)$$

where N indicates the number of simulations. The method was repeated increasing the number N of simulations and modifying the maximum degree p of the polynomials ψ_j , until E_{tot} was below the 5% for both the CNS (considering all tissues together) and the PNS. In the present paper, for both the models 49 simulations were necessary to satisfy this condition.

4. Analysis of the Exposure

Once the validation process was tested, each surrogate model was built for the CNS considering all the tissues together, for the PNS and for each single tissue that composed the CNS. Afterwards, as the computational effort in assessing the children exposure using PC models was very low, it was possible to evaluate a high number of coil positions and the corresponding E^{99th} in the tissues of interest. In particular, 10000 different coil positions were evaluated, in order to obtain the assessment of the exposure variability due to the near-field source position.

Furthermore, as it can be seen in step 4 of Fig.2, it was conducted a statistical analysis about the exposure variability. In specific, the Quartile Dispersion Coefficient (QDC) was calculated for every tissue as:

$$QDC = \frac{Q_3 - Q_1}{Q_3 + Q_1} \quad (6)$$

where Q_1 and Q_3 are, respectively, the first and third quartiles of the distribution E^{99th} .

Moreover, a global sensitivity analysis based on a variance-based method introduced by Sobol [37] was performed, in order to asses which input parameter of the three influenced most the output E^{99th} in each surrogate model. In detail, following the metric adopt in the work of Chiamarello et al [26], the variance of the system output was decomposed as a sum of each input parameters contribution and thus the Sobol indices were calculated as the ratios between the partial variances of the input parameters and the total variance of the system output. The Sobol indices were at the end normalized with respect to the sum of all the Sobol indices under consideration.

In the end, for PNS, for the whole CNS and for each tissue of CNS, an analysis of the source positions that induced E^{99th} values higher than the 70% of their maximum value was performed, for identifying the positions with major exposure risks.

III. RESULTS

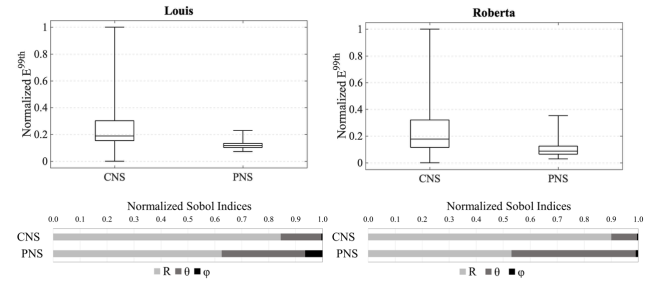


Fig. 3. The boxplots of the normalized E^{99th} in the upper part and the normalized Sobol indices found for E^{99th} in the lower part for the CNS and PNS tissues, in the left part for Louis model and in the right part for Roberta model. For the boxplots, the lower and upper bound of the box represent the first and the third quartiles, the line is the median value, and the whiskers are the minimum and maximum values.

In the upper part of Fig.3 there are displayed the boxplots of the normalized (between 0 and 1) E^{99th} values induced at the level of CNS and of PNS evaluating 10000 possible coil source positions, in the left part for Louis and in the right part for Roberta. Furthermore, in the lower part of Fig.3, there are also reported the normalized Sobol indices found in the CNS and in the PNS of the two different models.

As it can be seen from Fig. 3, the boxplots of the two models had a similar trend. In fact, the highest median and maximum obtained values are localized in the CNS respect to the PNS for both the models. The higher values in the CNS respect the PNS can be explained because in the analyzed exposure scenario the near-field source is indeed more in proximity to the CNS tissues (i.e. the child head) respect to the peripheral nerves of the PNS.

The statistical analysis, based on the QCD calculation, underlined that the exposure scenario was characterized in both the child models by a high variability depending on the near-field source position. In fact, the QCD values for the CNS were around 52% for Louis and around the 54% for Roberta, whereas for the PNS the QCD was a bit lower and it was equal to about 47% and about 45% for Louis and Roberta, respectively.

Furthermore, the similar trend in the exposure level of the two models was also confirmed in the analysis of the Sobol indices. The global sensitivity analysis showed in fact that the input parameter R influenced most the total system variability in the CNS of both models. More in details, the R parameter accounted in the CNS values around 84.5 % and 90.4 % of the total variability for Louis and Roberta, respectively. The input parameter θ was more relevant for the E^{99th} values of PNS of both models, the Sobol indices were in fact around 15% and 9.5% for the CNS, whereas for the PNS the values were around 31% and 46% for Louis and Roberta, respectively. At last, the input parameter ϕ remained almost uninfluential in both the tissues and models, its Sobol indices were in fact below 1% for the CNS cases, while for the PNS the parameter ϕ accounted the 6% and 1% of the total variability for Louis and Roberta, respectively.

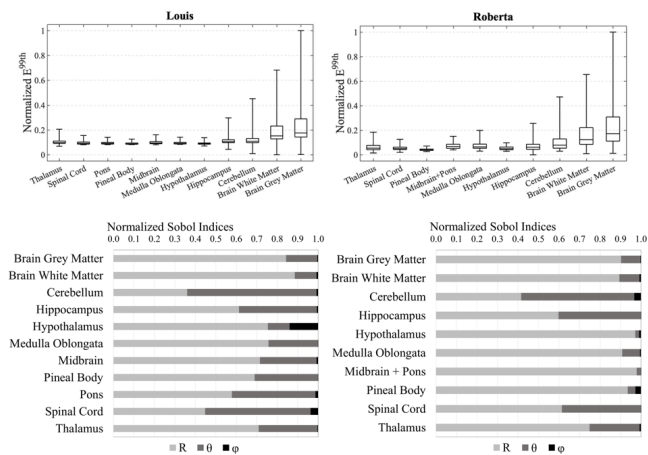


Fig. 4. The box plots of the normalized E^{99th} in the upper part and the normalized Sobol indices found for E^{99th} in the lower part for each tissue belonging to CNS, in the left part for Louis model and in the right part for Roberta model. For the boxplots, the lower and upper bound of the box represent the first and the third quartiles, the line is the median value, and the whiskers are the minimum and maximum values.

Fig. 4 shows the box plots of the normalized E^{99th} values induced in the CNS tissues for 10000 possible coil positions and the consequent global sensitivity analysis, on the left part for Louis and on the right part for Roberta. The similarity between the exposure trends of the two child models was found also in this case. For both the models, brain grey matter and brain white matter showed in fact the highest median and maximum values. This result was expected since these are the two tissues in the CNS that present the biggest area and are collocated in the most superficial part of the brain, closer to the near-field source. Furthermore, in both the models, the lowest median and maximum values were localized in pineal body and hypothalamus. These tissues represented on the contrary the smallest tissues, placed deep in the brain, and at higher distance from the source. Low median and maximum values were also obtained in both cases for spinal cord, which represented a tissue with an elongated shape spread in a direction far away to the near-field source.

The analysis of QDC values in the CNS tissues emphasized again that this exposure scenario was characterized by a high variability depending on the source position. The values of QDC varied in fact between a maximum value around to 53% for brain grey matter and a minimum value around to 37% for hippocampus in Louis, whereas for Roberta the QDC variation range is between 54% in brain white matter and 36% in spinal cord.

As it can be seen in the lower part of Fig.4, the global sensitivity analysis underlined that the input parameter that most influenced the exposure scenario in almost every CNS tissue was again R, which represented the distance between the child head and the coil. The variation of the Sobol indices for the parameter R considering all the tissues were in the range 88%-36% for Louis and in the range 90%-41% for Roberta. In particular, for both the models the parameter R influenced most the exposure level of brain grey matter and brain white matter, which are, as told before, the most

superficial tissues with the biggest area. The parameter R accounted in fact around 84% and 90% of the total variability for brain grey matter and around 88% and 89% for brain white matter for Louis and Roberta respectively. The input parameter θ resulted instead significantly relevant only for some specific tissues. In both the models, for example, cerebellum was influenced by this parameter. The Sobol indices resulted in fact around 63% and 55% for Louis and Roberta, respectively, showing that for this specific tissue the total variability was more characterized by the parameter θ than R. This can be explained by the tissue position in the head, cerebellum is in fact in the superficial part of the brain but only in the lower part of the head, so the angle θ can put the coil in proximity of this tissue and thus influencing the level of exposure. The same consideration is valid for spinal cord, which also resulted influenced by the θ parameter (values were around the 51% and 38% for Louis and Roberta). The first part of spinal cord is in fact positioned in the upper part of the neck, so coil positions due to the angle θ more near to that zone can greatly influence the exposure. Finally, the last input parameter ϕ was the one that influenced less the exposure level in both models. In some tissues its contribution was almost null (the variation range was in fact between 14% to below 1% for Louis and always below 1% for Roberta).

TABLE I

Variation range extremes of the three input parameters that induced in each tissue considered E^{99th} values higher than the 70% of the maximum value.

	LOUIS			ROBERTA		
	R	θ	ϕ	R	θ	ϕ
CNS	(120 mm, 132 mm)	(82°, 120°)	(-6°, 187°)	(120 mm, 132 mm)	(44°, 119°)	(11°, 190°)
PNS	(120 mm, 146 mm)	(67°, 120°)	(-10°, 190°)	(120 mm, 164 mm)	(104°, 120°)	(-8°, 177°)
Brain Grey Matter	(120 mm, 134 mm)	(81°, 120°)	(-6°, 190°)	(120 mm, 131 mm)	(38°, 120°)	(7°, 190°)
Brain White Matter	(120 mm, 133 mm)	(72°, 120°)	(14°, 190°)	(120 mm, 133 mm)	(51°, 120°)	(34°, 190°)
Cerebellum	(120 mm, 144 mm)	(98°, 120°)	(-6°, 173°)	(120 mm, 146 mm)	(89°, 120°)	(26°, 166°)
Hippocampus	(120 mm, 133 mm)	(93°, 120°)	(-8°, 187°)	(120 mm, 138 mm)	(91°, 120°)	(-9°, 190°)
Hypothalamus	(120 mm, 145 mm)	(-28°, 120°)	(-10°, 188°)	(120 mm, 136 mm)	(-30°, 120°)	(-10°, 190°)
Medulla Oblongata	(120 mm, 141 mm)	(69°, 120°)	(-9°, 189°)	(120 mm, 138 mm)	(61°, 120°)	(-9°, 189°)
Midbrain	(120 mm, 146 mm)	(93°, 120°)	(-10°, 190°)			
Pons	(120 mm, 145 mm)	(88°, 120°)	(-10°, 190°)	(120 mm, 134 mm)	(-30°, 120°)	(-10°, 190°)
Pineal Body	(120 mm, 136 mm)	(62°, 120°)	(-10°, 190°)	(120 mm, 140 mm)	(-28°, 119°)	(-10°, 190°)
Spinal Cord	(120 mm, 146 mm)	(80°, 120°)	(-9°, 189°)	(120 mm, 144 mm)	(78°, 120°)	(-8°, 190°)
Thalamus	(120 mm, 132 mm)	(95°, 120°)	(-10°, 189°)	(120 mm, 140 mm)	(84°, 120°)	(-10°, 190°)

In the end, to identify which were the source positions with an associated major exposure risks, it was conducted an evaluation of which, among the 10000 considered positions, induced E^{99th} values higher than 70% of their maximum value, for each tissue of CNS, for the whole CNS and for PNS in both models. The results of this analysis are reported in Tab.I. As it can be seen from Tab.I, in both models, the E^{99th} values higher than 70% of the maximum were found for all the tissues with source positions in proximity to the child head. The maximum values of the parameter R, which represented the distance between the head and the coil and could vary between 120 mm and 220 mm, were indeed 146 mm for Louis and 164 mm for Roberta. Another characteristic that could be noticed from Tab.I was that in both models and for almost every tissue,

the E^{99th} values higher than 70% of the maximum were localized in the head lower part of the sagittal plane. The lowest values of the parameter θ , which represented the rotation in the sagittal plane with a range between -30° and 120° , were in fact 62° for Louis, except for hypothalamus (values between -28° and 120°) and 38° for Roberta, except for hypothalamus, midbrain, pons and pineal body, where all the range of θ was covered. The position of the E^{99th} values higher than 70% of the maximum seemed not to be conditioned by the parameter ϕ , which represented the rotation in the transversal plane with a range between -10° and 190° . As it can be seen from Tab.1, for almost all the tissues and in both models the range of the parameter ϕ was in fact fully covered.

IV. DISCUSSION

The present work was focused on the assessment of children exposure variability due to a near-field source at 50 Hz varying the source position. The novelty of this work was the possibility to evaluate the exposure for a high number of source positions at low computational cost combining deterministic dosimetry with PC surrogate models, whereas in the previous studies [20-24] only worst-case scenarios were evaluated.

As a first finding, it was found that the maximum values of E^{99th} were localized in the CNS respect the PNS. Furthermore, the trend of the exposure levels for both CNS and PNS were almost equal across the two child models, even if the age range between the two models was wide, between five and fourteen years. When the analysis was conducted considering the E^{99th} in each CNS tissue, the results shown also in this case that the two models presented a similar exposure trend. The similarity of exposure levels in different child models was also found in the previous study of Chiramello et al. [26], who investigated on the electric fields induced in the same models when exposed to uniform magnetic fields at 50 Hz. This can be explained because, even if the height and the weight of the two models were evidently different, the sizes of CNS tissues were not so various. The variation of the brain grey matter volume between Roberta (i.e. the youngest child) and Louis (i.e. the oldest child) was indeed equal to only the 5%.

Furthermore, in both the cases, the highest median and maximum values of E^{99th} were found in the biggest tissues placed in the superficial part of the brain among those that composed the CNS, namely, in brain grey matter and in brain white matter. The lowest median and maximum values were found in hypothalamus and in pineal body, which are the smallest tissues considered, placed deep in the brain. These resulted are in line with the previous results of Cheng et al. [23], where it was shown that the induced currents in a model of human head using a small hand-held appliances were strongly dependent on the distance between the appliance and the head but also on the depth level of the tissues in the brain. Due to the rapid

decrease of the dipole magnetic field with distance, it was indeed expected that the tissues more superficial in the brain resulted exposed to higher level of magnetic fields. To reinforce again how much the coil position affected the exposure level of the different tissues, it was conducted the statistical analysis of the QDC value and the global sensitivity analysis on the three input parameters. The QCD values for both the child models were indeed between around 53% and 46% for CNS and PNS respectively. Furthermore, the global sensitivity analysis showed that the input parameter R, which described the distance between the head and the coil, was the one that most influenced the exposure level in all cases for CNS, for PNS and for all the CNS tissues. The input parameter θ was still quite relevant in the exposure, especially for some specific tissues (i.e. cerebellum, spinal cord and thalamus), where the position of the angle θ in the sagittal plane can greatly influence the results due to the morphological position of these tissues. These considerations highlighted that it was crucial to consider both parameters to obtain surrogate models able to reliably describe the exposure level in the different tissues. Regarding the last input parameter ϕ , it was noticed that it almost did not influence the exposure level in the tissues, so in the future analysis this parameter can be neglected in favor of the other two.

The analysis of which, among the 10000 considered source positions, induced E^{99th} values higher to 70% of the maximum value, confirmed and reinforced the considerations found from the global sensitivity analysis. In fact, the positions of the coil that caused the highest values of field were localized near to the head (12 cm to around 16 cm from the central point to the head) and more specifically in the lower head area of the sagittal plane (the variation range of θ is between 38° to 120° in the widest case). These results are in line with the work of Cheng et al. [23], where the use of a hairdryer at temple position caused higher level of exposure than using it on the head top. However, the cited study was limited in analyzing only two conditions, whereas with the present method it was possible to analysis a multitude of source positions to prove the results.

V. CONCLUSIONS

In conclusion, the evaluation of children exposure variability due to the near-field source changing source position and using stochastic dosimetry was achieved. The method was valid and seemed promising dealing with this type of exposure scenario, showing that this scenario is characterized by a high variability depending on the electric device position. The results added further knowledge about near-field source exposure. The method was in fact useful for individuating the source positions area that caused the highest exposure levels. It could be used in future dosimetry studies for addressing more on where to concentrate efforts for calculating the exposure level and for having a realistic characterization of the exposure assessment due to the use of electrical appliances.

ACKNOWLEDGMENT

The authors wish to thank the European project ARIMMORA (Advanced Research on Interaction Mechanisms of Electromagnetic Exposures with Organisms for Risk Assessment) (FP7-ENV-2011, Grant Agreement 282891, 2011–2014) and in particular the IT'IS Foundation for having provided the hairdryer data.

The authors wish to thank Schmid and Partner Engineering AG (www.speag.com) for having provided the simulation software SEMCAD X/SIM4Life.

REFERENCES

- [1] N. Wertheimer, E. Leeper, "Electrical wiring configurations and childhood cancer," *Am. J. Epidemiol.* 1979, 109, 273–284.
- [2] A. Ahlbom, N. Day and M. Feychting, "A pooled analysis of magnetic fields and childhood leukaemia," *British Journal of Cancer*, 2000, vol. 83(5), pp. 692–698.
- [3] S. Greenland, A.R. Sheppard, W.T. Kaune, C. Poole, M.A. Kelsh, "A pooled analysis of magnetic fields, wire codes, and childhood leukemia," *Childhood Leukemia-EMF Study Group. Epidemiology* 2000; 11: 624–634.
- [4] L. Kheifets, A. Ahlbom, C.M. Crespi et al., "Pooled analysis on recent studies on magnetic fields and childhood leukemia," *British Journal of Cancer*, 2010, vol. 103(7), pp. 1128–1135.
- [5] E. Steliarova-Foucher, C. Stillier, P. Kaatsch, F. Berrino, J.W. Coebergh, B. Lacour and M. Parkin, "Geographical patterns and time trends of cancer incidence and survival among children and adolescents in Europe since the 1970s (the ACCIS project): An epidemiological study," *Lancet*, 2004, 36, 2097–2105.
- [6] IARC Working Group on the Evaluation of Carcinogenic Risks to Humans. Non-Ionizing Radiation, Part 1: Static and extremely low frequency (ELF) electric and magnetic fields. In IARC Monographs on the Evaluation of Carcinogenic Risks to Humans; IARC Press: Lyon, France, 2002; Volume 80
- [7] U.M. Forssén, A. Ahlbom, M. Feychting, "Relative contribution of residential and occupational magnetic field exposure over twenty-four hours among people living close to and far from a power line," *Bioelectromagnetics* 2002, 23, 239–244.
- [8] D.E. Foliart, R.N. Iriye, J.M. Silva, G. Mezei, K.J. Tarr, K.L. Ebi, "Correlation of year-to-year magnetic field exposure metrics among children in a leukemia survival study," *J. Expo. Anal. Environ. Epidemiol.* 2002, 12, 441–447.
- [9] K.H. Yang, M.N. Ju, S.H. Myung, K.Y. Shin, G.H. Hwang, J.H. Park, "Development of a New Personal Magnetic Field Exposure Estimation Method for Use in Epidemiological EMF Surveys among Children under 17 Years of Age," *J. Electr. Eng. Technol.* 2012, 7, 376–383.
- [10] I. Calvente, C. Dávila-Arias, O. Ocón-Hernández, R. Pérez-Lobato, R. Ramos, F. Artacho-Cordón, N. Olea, M.I. Núñez, M.F. Fernández, "Characterization of indoor extremely low frequency and low frequency electromagnetic fields in the INMA-Granada cohort," *PLoS ONE* 2014, 5;9(9)
- [11] J. Schüz, C. Dasenbrock, P. Ravazzani, M. Rössli, P. Schär, P.L. Bounds, ... , N. Kuster, "Extremely low-frequency magnetic fields and risk of childhood leukemia: A risk assessment by the ARIMMORA consortium," *Bioelectromagnetics*, 2016, 37(3), 183–189. <https://doi.org/10.1002/bem.21963>
- [12] B. Struchen, I. Liorni, M. Parazzini, S. Gängler, P. Ravazzani, and M. Rössli, "Analysis of personal and bedroom exposure to ELF-MFs in children in Italy and Switzerland," *Journal of Exposure Science and Environmental Epidemiology*, 2016, vol. 26(6), pp. 586–596.
- [13] I. Liorni, M. Parazzini, B. Struchen, S. Fiocchi, M. Rössli, M., & P. Ravazzani, "Children's personal exposure measurements to extremely low frequency magnetic fields in Italy," *International Journal of Environmental Research and Public Health*, 13(6). 2016 <http://doi.org/10.3390/ijerph13060549>
- [14] I. Magne, M. Souques, I. Bureau, A. Duburcq, E. Remy, & J. Lambrozo, "Exposure of children to extremely low frequency magnetic fields in France: Results of the EXPERS study," *J. Expos. Sci. Environ. Epidemiol.*, 2017, 27(5), 505–512. <http://doi.org/10.1038/jes.2016.59>
- [15] N. Leitgeb, R. Cech, J. Schrottner, P. Lehofer, U. Schmidpeter, and M. Rampetsreiter, "Magnetic emissions of electric appliances," *Int J Hyg Environ Health*, 2008, 211: 69–73.
- [16] J. Schüz, J.P. Grigat, B. Stormer, G. Rippin, K. Brinkmann, and J. Michaelis, "Extremely low frequency magnetic fields in residences in Germany. Distribution of measurements, comparison of two methods for assessing exposure, and predictors for the occurrence of magnetic fields above background level," *Radiat Environ Biophys*, 2000, 39: 233–40.
- [17] F. Abuasbi, A. Lahham, and I.R. Abdel-Raziq, "Residential exposure to extremely low frequency electric and magnetic fields in the city of Ramallah-Palestine," *Radiation Protection Dosimetry*, 2018, 179(1):49-57. <https://doi.org/10.1093/rpd/ncx209>
- [18] E.A. Ainsbury, E. Conein, E., and D.L. Henshaw, "An investigation into the vector ellipticity of extremely low frequency magnetic fields from appliances in UK homes," *In Phys Med Biol*, 2005, 3197-209.
- [19] T. Behrens, C. Terschuren, W.T. Kaune, and W. Hoffmann, "Quantification of lifetime accumulated ELF-EMF exposure from household appliances in the context of a retrospective epidemiological case-control study," *In J Expo Anal Environ Epidemiol*, 2004, 144-53.
- [20] S. Tofani, et al. "Electric field and current density distributions induced in an anatomically-based model of the human head by magnetic fields from a hair dryer," *Health physics*, 1995, 68.1: 71–79.
- [21] L.E. Zaffanella, T.P. Sullivan, & I. Visintainer, "Magnetic field characterization of electrical appliances as point sources through in situ measurements," *IEEE transactions on power delivery*, 1997, 12(1), 443–450.
- [22] S. Nishizawa, F.M. Landstorfer, Y. Kamimura, "Low-frequency dosimetry of inhomogeneous magnetic fields using the coil source model and the household appliance," *IEEE transactions on biomedical engineering*, 2007, 54.3: 497–502.
- [23] J. Cheng, et al., "Magnetic field induced currents in a human head from use of portable appliances," *Physics in Medicine & Biology*, 1995, 40.4: 495.
- [24] A. Christ, R. Guldemann, B. Buhlmann, M. Zefferer, J.F. Bakker, G.C. van Rhoon, et al., "Exposure of the human body to professional and domestic induction cooktops compared to the basic restrictions," *In Bioelectromagnetics*, 2012, 695–705.
- [25] I. Liorni, M. Parazzini, S. Fiocchi, and P. Ravazzani, "Study of the influence of the orientation of a 50-Hz magnetic field on fetal exposure using polynomial chaos decomposition," *International Journal of Environmental Research and Public Health*, 2015, vol. 12, no. 6, pp. 5934–5953.
- [26] E. Chiaramello, S. Fiocchi, P. Ravazzani and M. Parazzini, "Stochastic dosimetry for the assessment of children exposure to uniform 50 Hz magnetic field with uncertain orientation," *BioMed research international*, 2017.
- [27] E. Chiaramello, M. Parazzini, S. Fiocchi, P. Ravazzani and J. Wiart, "Assessment of fetal exposure to 4g lte tablet in realistic scenarios: Effect of position, gestational age, and frequency," *IEEE Journal of Electromagnetics, RF and Microwaves in Medicine and Biology*, 2017, 1(1), 26-33.
- [28] N. Wiener, "The homogeneous chaos," *American Journal of Mathematics*, 1938, vol. 60, no. 4, pp. 897–936.
- [29] ICNIRP. 2010. ICNIRP guidelines for limiting exposure to time-varying electric and magnetic fields (1 Hz - 100 kHz). *Health Physics*, 99(6):818-836.
- [30] M.-C. Gosselin, E. Neufeld, H. Moser et al., "Development of a new generation of high-resolution anatomical models for medical device evaluation: The Virtual Population 3.0," *Physics in Medicine and Biology*, 2014, vol. 59, no. 18, pp. 5287–5303.
- [31] G. Blatman, "Adaptive sparse polynomial chaos expansions for uncertainty propagation and sensitivity analysis". PhD thesis, Université Blaise Pascal, Clermont-Ferrand, 2009.
- [32] C. Gabriel, S. Gabriel and Y.E. Corthout, "The dielectric properties of biological tissues: I. Literature survey," *Physics in Medicine & Biology*, 1996, 41(11), 2231.
- [33] C. Gabriel, A. Peyman and E.H. Grant, "Electrical conductivity of tissue at frequencies below 1 MHz," *Physics in medicine & biology*, 2009, 54(16), 4863.

- [34] I. Liorni, M. Parazzini, S. Fiocchi et al., "Dosimetric study of fetal exposure to uniform magnetic fields at 50 Hz," *Bioelectromagnetics*, 2014, vol. 35, no. 8, pp. 580–597.
- [35] B. Efron, T. Hastie, I. Johnstone and R. Tibshirani, "Least angle regression," *The Annals of statistics*, 2004, 32(2), 407-499.
- [36] S. Marelli and B. Sudret, "UQLab: A framework for uncertainty quantification in Matlab," In *Vulnerability, Uncertainty, and Risk: Quantification, Mitigation, and Management*. 2014, (pp. 2554-2563).
- [37] I. M. Sobol, "Global sensitivity indices for nonlinear mathematical models and their Monte Carlo estimates," *Mathematics and Computers in Simulation*, 2001, vol. 55, no. 1-3, pp. 271–280.



Paolo Ravazzani(M'14) received the master's degree in electronic engineering and the Ph.D. degree in bioengineering, both from Politecnico di Milano, Milan, Italy. He is currently the Director of research with the Consiglio Nazionale delle Ricerche, Institute of Electronics, Computer and Telecommunication Engineering. His main research interests include exposure assessment of electromagnetic fields related to the study of the possible effects of electromagnetic fields on health and biomedical applications of electromagnetic fields.



Marta Bonato received the master's degree in biomedical engineering from the Polytechnic of Milan, Milan, Italy, in July 2017, where she is currently working toward the Ph.D. degree in bioengineering. From September 2017 to April 2018, she was with the Institute of Electronics, Computer and Telecommunication Engineering, Consiglio Nazionale delle Ricerche, as a Research Fellow. Her research interests are related to the

study of the interaction of electromagnetic fields (EMF) with biological systems and the study of possible effects of EMF on health.



Marta Parazzini (M'04) is a Research Scientist with the Institute of Electronics, Computer, and Telecommunication Engineering, Italian National Research Council, Milan, Italy. Her primary research interests include the medical applications of EMF, in particular the techniques for noninvasive brain stimulation, the study of the interactions of EMF with biological systems, and deterministic and stochastic computational dosimetry.



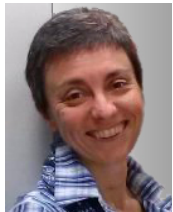
Emma Chiaramello received the master's and Ph.D. degrees in biomedical engineering from the Politecnico di Torino, Torino, Italy, in 2009 and 2013, respectively. She is a Postdoctoral Research Fellow with the Institute of Electronics, Computer and Telecommunication Engineering, National Research Council of Italy. Her scientific interests

include the study of the interactions between EMF and biological systems, with both deterministic dosimetry based on computational electromagnetism methods and stochastic dosimetry based on surrogate modeling.



Serena Fiocchi received the master's degree in biomedical engineering in 2009 and the Ph.D. degree in bioengineering in 2014, both from the Polytechnic of Milan, Milan, Italy. She is a Research Scientist with the Institute of Electronics, Computer and Telecommunication Engineering, National Research Council of Italy. Her scientific interests

include the study of the computational modeling of noninvasive brain and spinal stimulation techniques, the design and the optimization of biomedical technologies based on electromagnetic fields (EMF) for diagnostic and therapeutic applications, and the computational modeling of the interactions between EMF and biological systems.



Gabriella Tognola received the master's degree in electronic engineering and the Ph.D. degree in bioengineering, both from Politecnico di Milano, Milan, Italy. She is currently Senior Research Scientist with the Consiglio Nazionale delle Ricerche, Institute of Electronics, Computer and Telecommunication Engineering. Her main research interests include exposure assessment of electromagnetic fields with

numerical dosimetry and with Machine Learning methods and modelling of electromagnetic fields for biomedical applications.